ACS OMEGA

Open Access

http://pubs.acs.org/journal/acsodf

Article

Sprayable Biocide-Free Polyurethane Paint that Reduces Biofouling and Facilitates Removal of Pathogenic Bacteria from Surfaces

Lawrence M. Chen,[‖] La'Darious J. Quinn,[‖] Jordan T. York, Thomas J. Polaske, Alexandra E. Nelson, Visham Appadoo,* Cornelius O. Audu,* Helen E. Blackwell,* and David M. Lynn*

Cite This: *ACS Omega* 2025, 10, 7295−7305

Read Online

ACCESS | Metrics & More | Article Recommendations | Supporting Information

ABSTRACT: The ability to prevent bacterial adhesion on surfaces and to facilitate the removal of bacteria once they have already contaminated or colonized a surface is important in a broad range of fundamental and applied contexts. The work reported here sought to characterize the physicochemical properties of a family of biocide-free hydrophobic polyurethane coatings containing polysiloxane segments and evaluate their ability to mitigate bacterial fouling and/or facilitate subsequent surface cleaning after exposure to pathogenic bacteria. We developed benchtop microbiological assays to characterize surface fouling and subsequent removal of bacteria after repeated (i) short-term intermittent physical contact with and (ii) longer-term continuous flow-based contact with liquid growth media containing either *S. aureus* or *E. coli*, two common Gram-positive or Gram-negative bacterial pathogens, respectively. Characterization of fouled and cleaned surfaces using fluorescence microscopy and standard agar-based plaque assays revealed significant differences in both reductions in initial fouling and subsequent cleanability after gentle rinsing with water. These differences correlated to differences in the surface properties of these materials (e.g., hydrophobicity and contact angle hysteresis), with coatings exhibiting lower contact angle hysteresis generally having the greatest antibiofouling and easy-to-clean properties. Our results suggest that these biocide-free, siloxane-containing polyurethane-based clearcoat materials show significant promise for the mitigation of surface fouling and bacterial adhesion, which could prove useful in a range of commercial applications, including in "high touch" environments where microbial contamination is endemic.

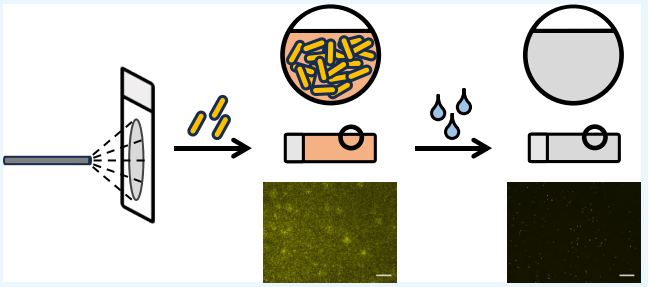

INTRODUCTION

Coatings that contain antibacterial agents can be highly effective at reducing or preventing biofouling on surfaces. Many different types of biocidal coatings are currently in commercial use or are being developed for new applications, for example, to prevent fouling and infection on the surfaces of implantable biomedical materials in clinical applications[1−6] or to prevent biofouling on the hulls of seafaring vessels that can increase drag and associated transportation costs.[3,7−10] These coatings often contain components that disrupt biological function either through direct contact with microorganisms at the surface or by the controlled release of biocidal compounds, including antibiotics (e.g., chlorhexidine, triclosan, and gentamicin), metal-containing compounds (e.g., tributyltin, cuprous oxide, and zinc oxide), silver nanoparticles, cationic polymers, or quaternary ammonium/phosphonium salts.[1−14] While these strategies can be effective at preventing the colonization of surfaces by microorganisms, recent years have seen increasing regulatory pressure to limit the use, or potential overuse, of biocides.[8,10,15] These concerns are motivated, at least in part, by potential negative impacts that the leaching of biocides can have on other cells and organisms in surrounding environments.[8,10,16−18]

As potential alternatives to biocidal coatings, several different types of biocide-free or so-called "passive" antibiofouling approaches have been developed. These approaches typically exploit strategies that involve modifications to surface chemistry or nano/microscale surface topography, and include various types of superhydrophobic surfaces,[19] liquid-infused surfaces,[20,21] and so-called "fouling-release" coatings[8,10] that can either (i) reduce the initial adhesion of bacteria and other biofoulants or (ii) reduce the effort required to remove them once they are adhered.[1,3,8,10,15,19−29] As one example, Privett et al. demonstrated that a superhydrophobic coating comprising fluorinated colloids and fluorinated resins can reduce the adhesion of *Staphylococcus aureus* and *Pseudomonas aeruginosa*, two common and often deadly opportunistic bacterial pathogens.[30] More recently, Esmeryan[31,32] and others[33] have used strategies for the fabrication of topographically complex

Received: December 5, 2024
Revised: January 22, 2025
Accepted: January 29, 2025
Published: February 12, 2025

and water-repellant carbon soot-based coatings that exhibit antibiofouling behaviors in laboratory[32,33] and real-world[31] environments. It is worth noting that, while these and many related approaches represent significant advances toward the design of biocide-free antibiofouling coatings, many of these strategies also make use of fluorinated polymers,[30] oils,[20,21] and/or treatments with other fluorinated agents[31−33] during or after assembly to help achieve their low-energy surface properties. Recent regulatory concerns around the use of per- and polyfluoroalkyl substances (PFAS) have also inspired renewed interest in the pursuit of "passive" strategies for the design of low surface energy antifouling coatings that are both biocide-free and not prepared using highly fluorinated materials.[8,10,34−38] Many silicone-based fouling-release coatings are emblematic of this general approach[8,10] and provide design principles and guidance useful for the design of new antibiofouling materials.

Our laboratories have long-term interests in the development of hydrophobic and slippery materials and surface coatings that are intrinsically resistant to microbial fouling.[39−50] As part of ongoing collaborative efforts to develop polymer-based coatings to protect or enhance the appearance of commercial assets, we recently disclosed the design of a family of hydrophobic and PFAS-free "Easy-to-Clean" (E2C) polyurethane coatings.[51,52] These E2C coatings exhibit low surface energies, high hydrophobicity, and low coefficients of friction typically associated with fluorinated materials and can reduce the effort needed to clean surfaces fouled with a broad range of substances, including dirt and many different types of commercial liquids, gels, and other environmental contaminants. The work reported here sought to determine the extent to which these hydrophobic and biocide-free E2C coatings could reduce initial bacterial adhesion and/or provide polymer-coated surfaces that are easy to clean after bacterial biofouling.

In this paper, we report the physicochemical properties of a family of hydrophobic polyurethane-based coatings containing polysiloxane segments of different length and structure and their performance in mitigating bacterial adhesion after repeated exposure to two common bacterial pathogens. We developed a series of assays to characterize surface fouling and subsequent cleanability after repeated (i) short-term intermittent physical contact with and (ii) longer-term continuous flow-based contact with liquid growth media containing either Gram-positive or Gram-negative bacteria (*S. aureus* or *Escherichia coli*, respectively). Characterization of fouled and cleaned surfaces using fluorescence microscopy and standard agar-based plaque assays revealed significant differences in both reductions in initial fouling and subsequent cleanability after gentle rinsing with water that correlate to differences in the surface properties of these materials (e.g., hydrophobicity and contact angle hysteresis). Our results suggest that these siloxane-containing polyurethane coatings show promise for mitigation against surface fouling and bacterial adhesion, which could be leveraged in commercial uses and other applied contexts (e.g., "high touch" surfaces) for which microbial contamination is widespread. In addition, the benchtop microbial assays reported here could, with further development, provide a basis for the development of high-throughput methods for the characterization and identification of other types of antibiofouling or readily cleanable coatings.

MATERIALS AND METHODS

Materials. Ethanol was obtained from Decon Laboratories (King of Prussia, PA). Water (18 MΩ) was purified using an ARIUM Pro ultrapure water system (Sartorius). FISHERFINEST premium microscope slides (Cat. No. 22-038-013) were obtained from Fisher Scientific (Hampton, NH). Brain heart infusion (BHI) broth medium was obtained from Teknova (Hollister, CA). Lennox L Broth (LB) medium was obtained from Research Products International (Mt. Prospect, IL). Freezer stocks of *S. aureus* YFP fluorescent strain (gift of Alexander Horswill; AH1677)[53] were maintained in 1:1 BHI broth:glycerol (50% v/v in Milli-Q water). Stocks of *E. coli* GFP fluorescent strain (obtained from ATCC; 25922GFP) were maintained in 1:1 LB medium:glycerol (50% v/v in Milli-Q water) at −80 °C. Standard laboratory cotton-tipped applicators were purchased from Puritan Medical Products. All materials were used as received without further purification unless otherwise noted. All experiments were performed in at least triplicate unless otherwise indicated.

Instrumentation and Data Analysis. Surface property measurements were obtained using a Krüss DSA100 instrument equipped with ADVANCE software, which provides an automated interface for collecting static water contact angles (sWCA), dynamic water contact angles (dWCA), and surface free energy (SFE). Image and optical settings employed for these measurements were as follows: illumination = 90; camera shutter time = 82; zoom = 59; focus = 17; frame rate = 50. Using the sessile drop method in ADVANCE, sWCAs were measured by depositing a 2.0 μL drop of probing liquid (i.e., water and diiodomethane) on the surface of a substrate. Baseline correction was automated except for certain cases (e.g., glossy surfaces) where fitting to the droplets was performed manually for greater accuracy. Droplets of diiodomethane were used to determine SFE using the Owens-Wendt method.[54] Polar and dispersive surface energy values were also calculated using ADVANCE; to facilitate sample-to-sample comparisons, the polar component of surface energy was represented as a percentage of the total surface energy of that coating (% polar component). Dynamic water contact angles were determined by measuring advancing and receding contact angles, obtained by either moving the needle into the middle of the drop and "dosing" (for advancing) or "aspirating" (for receding) a drop. A delay time of 8 s was set between each action (i.e., dosing a drop, measurement, or aspirate) to ensure complete equilibration of the drop prior to measurement. Drop shapes were fit to a Tangent model in which only the right contact angle of the drop could be measured consistently and accurately. Hysteresis was then calculated as the difference between the advancing and receding angles. Digital photographs were acquired using a Samsung Galaxy S20 smart phone. All numerical data were analyzed and plotted using GraphPad Prism software (v. 9.0.0.).

Synthesis of Polyurethane Clearcoats and Preparation of Polymer-Coated Surfaces. Glass slides coated with polyurethane-based clearcoats were prepared by PPG in a manner similar to published methods.[55,56] Hydroxyl-terminated acrylate polyols were synthesized by the free radical polymerization of monomer mixtures comprising desired ratios of cyclic and/or linear aliphatic methacrylates, aryl methacrylates, (hydroxyethyl)methacrylates, and/or styrene monomers. To a reaction vessel, the resulting monomer mixtures were slowly combined (over 3 h) with a peroxide-based

https://doi.org/10.1021/acsomega.4c11020
ACS Omega 2025, 10, 7295−7305

Table 1. Materials Characterization Data for the Surface Coatings Used in This Study

sample	θ_{stat} (deg)	θ_{adv} (deg)	θ_{rec} (deg)	θ_{hys} (deg)	TSE (mN/m)	% polar	T_g (°C)
AS1	83.2 ± 1.6	91.5 ± 0.3	51.6 ± 0.3	39.9 ± 0.5	42 ± 2	6 ± 1	69
AS2	89.5 ± 1.6	91.4 ± 0.2	66.8 ± 0.3	24.6 ± 0.5	34 ± 3	6 ± 2	89
AS3	105.9 ± 0.3	107.4 ± 0.8	102.8 ± 1.3	4.7 ± 1.9	18 ± 0.3	5 ± 0.3	71
AS4	105.4 ± 0.9	108.3 ± 1.3	97.2 ± 1.7	11.1 ± 0.5	20 ± 1	4 ± 1	105

initiator and an aromatic solvent (e.g., toluene, xylene) and subsequently refluxed for at least 1 additional hour. The resulting acrylic polyol was then characterized by gel permeation chromatography[57] and polyol titration[58] to determine molecular weight (MW) relative to polystyrene standards and hydroxyl value on solids, respectively. As such, the associated acrylate polyol featured in **AS1** control coatings has a MW = 6200−6500, OH value (*s*) = 120−155, T_g = 2−5 °C (as predicted by the Fox Equation)[59,60] and an overall nonvolatile content of 57−65% by wt. The resulting acrylic polymer resins were subsequently mixed with a commercial aliphatic isocyanate cross-linker resin (DESMODUR N 3300A) and a blend of additives in acetate solvents to control coating rheology, flow, and surface energy. This mixture was then diluted further with acetate solvents to reach a viscosity of ∼40 cP sufficient for spray-based application. The final mixture used to synthesize clearcoat **AS1** was composed of 55% total solids by weight and 45% solvent mixtures, consistent with established standards for polyurethane automotive clearcoat formulations.[55] Clearcoats **AS2−4** were prepared in a similar method as described above with the exception that small amounts of reactive proprietary acrylic additives with polysiloxane side groups were co-blended into clearcoat formulations to achieve the differentiated surface and physicochemical properties shown in Table 1.

For the coating of all samples used in this study, glass microscope slides were mounted onto steel substrates using masking tape and the exposed surfaces of the slides were then wiped clean using isopropanol and KIMTECH precision wipes. Eight of these sample-loaded steel substrates were then mounted on a sample holding unit attached to a COMPU-SPRAY Automatic Test Panel Spray Machine (Standard 310940, Spraymation, Ft. Lauderdale, FL). This approach enabled automated liquid coating application to generate 72 coated samples using different polyurethane coatings. Samples were then placed on a horizontal rack and allowed to air-dry for 10 min before baking for 30 min at a cure temperature of 140 °C. Coated samples were then removed from the backing steel substrate, packaged into a microscope slide box, and stored in the dark and at ambient temperature prior to use.

Characterization of Anti-Biofouling Behavior of Polymer-Coated Surfaces (Fluid Flow Assay). Overnight cultures of bacteria were grown in 50 mL BHI medium + 10 μg/mL chloramphenicol (for *S. aureus* AH1677) or 50 mL LB medium + 100 μg/mL ampicillin (for *E. coli* 25922GFP) at 37 °C with shaking at 200 rpm. Prior to inoculation with bacterial cultures, coated glass substrates were sterilized with a 70% ethanol:water solution and allowed to air-dry at ambient temperature. The sterilized substrates were then placed on a home-built sample stage positioned at a 10° incline and housed inside a biosafety cabinet (BSC) at ambient laboratory temperature. The open ends of 1/16″ Tygon tubing connected to a Watson-Marlow 120S/DM3 peristaltic pump were positioned approximately 2 cm below the top edge of each substrate, and a 25 mL volume of the overnight culture of bacteria was continuously passed through the tube and allowed to flow from the top to the bottom along the center of each sample at a rate of 50 rpm (∼5 mL/min). A sterile basin (Corning Costar 50 mL reagent reservoir) positioned at the bottom of the sample stage collected the fluid and the fluid was recycled to the pump for continuous passage over the sample. After 3 h, the substrates were removed, allowed to air-dry, and exposed to illumination from a built-in UV lamp (UVC, 200−280 nm) inside the BSC for 15 min for sterilization. Substrates were then placed in covered Petri dishes, removed from the BSC, and imaged using an Olympus IX70 inverted microscope (Center Valley, PA) and a QImaging EXi Aqua camera (Tucson, AZ) at 20× magnification. GFP or YFP produced in the bacteria was excited with a Lumen Dynamics X-CITE Series 120PC-Q fiber-coupled mercury lamp (Monroe, LA) using the GFP channel to facilitate visualization.

To quantify the degree of fouling for each substrate, the metric of corrected total cell fluorescence (CTCF) was calculated. Briefly, for each individual substrate, at least 30 images were acquired in the fouled region on the surface and in areas that were not exposed to flow and did not exhibit visible fluorescence. The latter images were used to subtract background signal. Mean gray values of background images, total image area, and integrated densities of fouled images were calculated using the image processing software package ImageJ 1.52a. The mean gray values of background images were then averaged to obtain a mean fluorescence of background value for each substrate. These values were used to calculate CTCF for each fouled image using the following equation:

$$\text{CTCF} = [\text{Integrated Density}] - [\text{Total Image Area} \times \text{Mean Fluorescence of Background}]$$

The median CTCF value for each substrate was then calculated and is reported in this study.

After imaging, samples were cleaned by submerging substrates completely into four separate 200 mL volumes of fresh deionized water in a glass beaker. Samples were held under water and without additional agitation for 5 s during each clean cycle. The samples were then allowed to air-dry under ambient conditions on the lab benchtop, and then imaged again using fluorescence microscopy to characterize post-washing changes in fluorescence intensity. For experiments in which samples underwent multiple rounds of the fouling and cleaning steps described above (see text), cleaned substrates were subjected to iterative fouling and cleaning steps using freshly prepared overnight cultures of bacteria for each fouling step using the procedures described above, with the exception of the initial 70% ethanol wash.

Characterization of Antibiofouling Behavior of Polymer-Coated Surfaces (Swabbing Assay). Overnight cultures of *S. aureus* AH1677 were grown in 3 mL BHI medium +10 μg/mL chloramphenicol at 37 °C with shaking at 200 rpm. After 20 h of growth, the culture was diluted 1:1000 in BHI to yield a final volume of 50 mL. Substrates used in

https://doi.org/10.1021/acsomega.4c11020
ACS Omega 2025, 10, 7295−7305

Scheme 1. Schematic Illustration Showing the Generalized Polymer Network Structures of Polyurethane-Based Clearcoats AS1−AS4 Investigated in This Study[a]

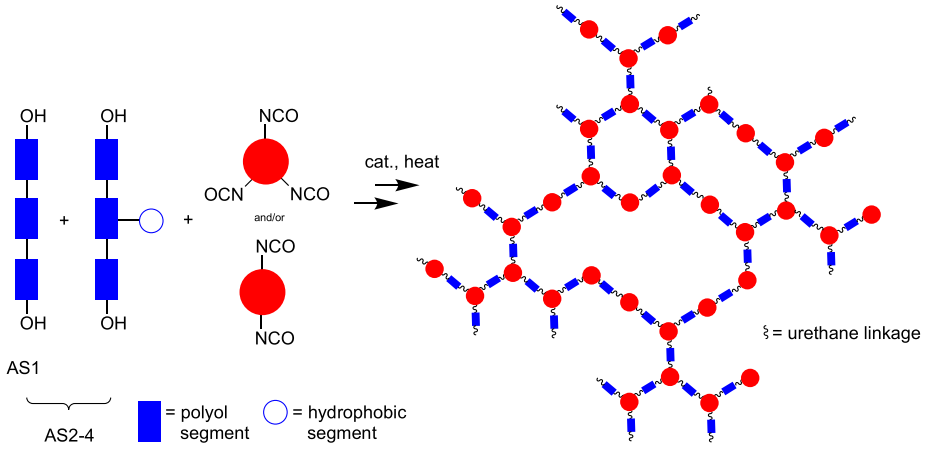

[a]These polyurethane clearcoats were synthesized using strategic combinations of (i) hydroxyl-containing polyols (depicted in blue) containing or not containing pendant polysiloxane-based segments (depicted as a white open circle) and (ii) mixtures of di- and triisocyanates (depicted as filled red circles). Polyols end-capped with hydroxyl groups can react with isocyanate trimers or dimers to form a polyurethane network (right) in the presence of heat and an appropriate catalyst (black squiggles represent polyurethane linkages). **AS1** was synthesized using the polyol without the hydrophobic segment. For **AS2−4**, a combination of both polyols were used and the proprietary hydrophobic polysiloxane segment was varied in ways that led to varying surface properties as shown in Table 1 and discussed in the main text. See Materials and Methods for additional details relating to the synthesis and characterization of these materials.

swabbing-based inoculation experiments were cut into 2.5 × 2.0 cm^2 samples and then sterilized using a 70% ethanol:water solution and dried prior to use. Surfaces were inoculated by soaking a standard laboratory cotton-tipped applicator in the diluted *S. aureus* AH1677 culture for 5 s and then manually rubbing the applicator in roughly 1.5 cm diameter circles at the center of the surface of each sample for 10 s in a BSC. This process was repeated a total of 10 times using a new applicator for each inoculation. No-bacteria control samples were prepared using this same procedure, with the exception that the applicators were dry. After 10 rounds of swabbing, samples exposed to bacteria were divided into two groups, one of which was cleaned by manually passing five 1 mL volumes of sterilized Milli-Q water gently over the sample surface via an Eppendorf Research Plus micropipette ("cleaned samples") held with sterilized forceps at an angle of ∼90°, and one that received no additional treatment ("dirty samples"). No-bacteria control samples were also cleaned using this gentle washing procedure. Using sterilized forceps, each set of samples was then placed coating-side-down on agar gel (1.5% (w/v) agar in BHI + 10 μg/mL chloramphenicol) in a 10 cm diameter Petri dish (3 samples per plate) for 5 min. After 5 min, the samples were removed, and the agar gel plates were placed in an incubator at 37 °C. Digital photographs of the agar plates were acquired after 16 h of incubation to analyze bacterial growth on the agar surface on which the samples were placed.

Quantification of the degree of fouling for each substrate was achieved by measuring the percentage of the total substrate area covered by *S. aureus*. To accomplish this, the images of the agar gels taken at 16 h were cropped to the individual substrate for each substrate type (3 total images) using Windows Photo Viewer. These images were further processed to binary (black/white) images, with the black areas corresponding to *S. aureus* coverage and the white being background, using ImageJ software. The calculation of percent area covered was achieved by dividing the total area of *S. aureus* coverage by the area of the substrate (5 cm^2) and multiplying the quotient by 100 to give the results shown in the main text.

RESULTS AND DISCUSSION

Preparation of Hydrophobic Polyurethane-Based Coatings. All studies described below were conducted using four polymer coatings (referred to from here on as coatings **AS1−AS4**) comprising proprietary formulations of polyurethane-based clearcoat resins with systematic variations in the structure and molecular weights of incorporated polysiloxane-based segments. Scheme 1 provides a schematic illustration of the cross-linked polyurethane-based clearcoats investigated here, synthesized using strategic combinations of (i) polyol segments (either containing or not containing pendant polysiloxane-based segments) and (ii) mixtures of di- and triisocyanates (see Materials and Methods for additional details relating to the synthesis and characterization of these materials). **AS1** is a standard model polyurethane-based clearcoat developed by PPG Industries that contains no polysiloxane-based segments; **AS2**, **AS3**, and **AS4** were structurally similar to **AS1**, with the exception that the resulting coatings also contained lower (**AS2**) and higher (**AS3** and **AS4**) amounts of hydrophobic polysiloxane segments. All coatings were fabricated using spray-based methods on standard glass microscope slides. Table 1 summarizes key surface properties (static and dynamic water contact angles, contact angle hysteresis, and the total surface energy (TSE) and percent polar component of the surface energy) and other physical properties (glass transition temperature) measured experimentally for all four coatings used in this study. Of note, coatings **AS3** and **AS4** exhibited higher water contact angles and substantially lower contact angle hystereses and total surface energies, consistent with the greater amount of hydrophobic polysiloxane segments in these samples. We return to these observations again in the discussion below.

https://doi.org/10.1021/acsomega.4c11020
ACS Omega 2025, 10, 7295−7305

Short-Term Touch-Based Bacterial Fouling and Cleaning Assays. In a first series of experiments, we sought to characterize the ability of coatings **AS1**−**AS4** to resist bacterial fouling and enable straightforward cleaning with minimal effort after intermittent and repeated short-term contact with liquid growth media containing bacteria. We selected the Gram-positive bacterium *S. aureus* for these initial studies because it is a common pathogen and frequent colonizer of human skin and inanimate surfaces, and our laboratories have broad experience in its culture and manipulation.[42,43,45,47,61,62] Guiding our development of these methods was the desire to generate protocols that are (i) relevant to types of surface contamination events that can occur in everyday life, (ii) simple to perform in a standard laboratory equipped for biological experimentation, and (iii) readily amenable to testing with other bacterial and/or fungal cell types. We developed a swab-based contact-transfer assay to safely mimic repeated and short-term touch-based contact with surfaces coated with **AS1**−**AS4** (Figure 1A, top). For these and all other studies described below, we adopted gentle rinsing with water containing no detergents or surfactants, followed by touch-free air drying at ambient temperature, as a straightforward and non-aggressive (or minimally aggressive) means to evaluate easy-to-clean properties (see Materials and Methods for additional details).

For each experiment, glass slides coated with **AS1**−**AS4** were inoculated 10 times using a cotton-tipped applicator soaked in growth media containing *S. aureus* AH1677 and then either (i) rinsed in water and dried ("cleaned samples") or (ii) immediately dried without rinsing in water ("dirty samples"). These samples were then inverted and placed briefly on agar plates to assess and compare (i) differences in levels of initial bacterial contamination (dirty samples) and (ii) the relative amounts of bacteria remaining on each coated surface after gentle washing (cleaned samples; e.g., see schematic in Figure 1A, bottom).

Figure 1B shows representative images of agar plates inoculated with cleaned and dirty samples of **AS1**−**AS4** after 16 h of incubation (the blue lines in these images mark the areas where the rectangular coated samples were placed during inoculation and are included to guide the eye). Inspection of these images reveals large differences in the levels of bacteria growing on the agar contacted with dirty samples and cleaned samples (in these images, areas containing *S. aureus* colonies appear as darker gold-colored spots; areas devoid of *S. aureus* are lighter in color and similar to the areas of background outside the blue boxes). We conclude based on these qualitative images that all samples were robustly contaminated using the iterative, swab-based contact-transfer method used here, and that all samples were substantially cleaned after gentle rinsing with water. Additional images of individual samples from this experiment, the results of additional no-bacteria controls, and images from multiple independent trials are included in Figures S1−S3.

We used image processing software to quantify the percent areal coverage of bacterial colonies on agar plates in the areas inoculated by each coated substrate. The results of this analysis are shown in Figure 1C and reveal large and statistically relevant differences in areal coverage on dirty samples (black bars) relative to samples that were subsequently cleaned (white bars). Further inspection of this plot shows that samples coated with **AS1** exhibited lower levels of initial fouling relative to **AS2**−**AS4** after initial contact with bacterial cultures. The

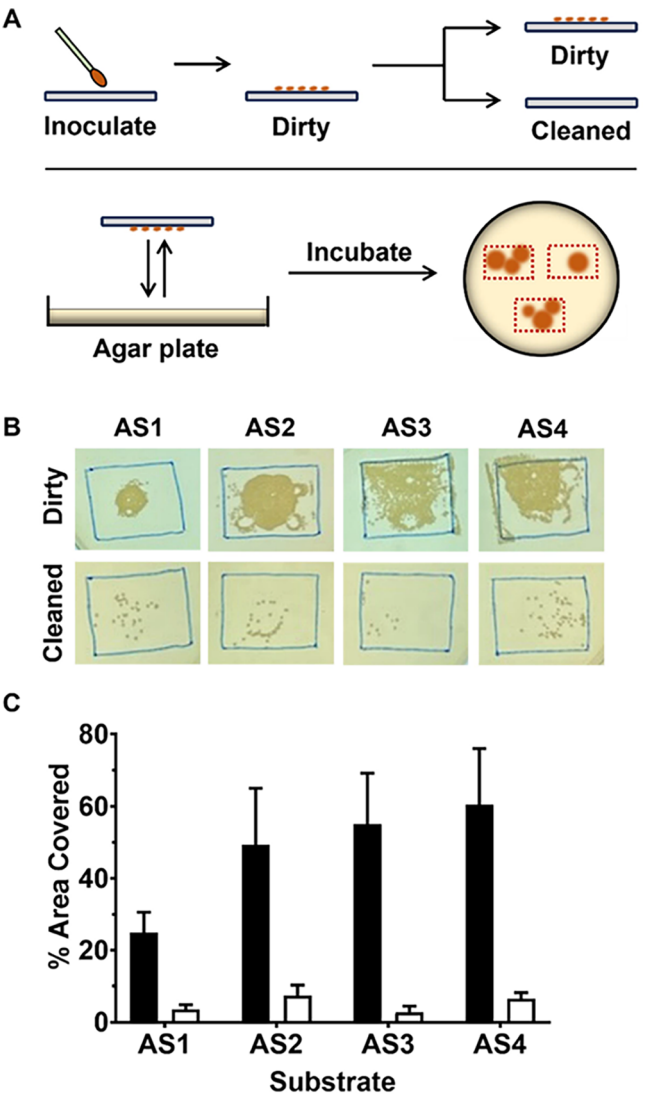

Figure 1. (A) Top: Schematic showing the overall scheme used for the physical, touch-based inoculation and subsequent cleaning of polymer-coated glass substrates. Bottom: Schematic showing agar-based assay used to characterize bacterial fouling on substrates before or after cleaning. (B) Representative images of bacterial growth on agar plates after contact with inoculated surfaces (top row) or surfaces that were inoculated and then subsequently cleaned prior to analysis (bottom row). Photos were taken after 16 h of incubation. Hand-drawn blue rectangles are 2.5 × 2.0 cm^2 and denote the locations in which coated substrates were briefly placed on the agar; these markings are included to guide the eye (see text for additional details). (C) Average percentage of bacterial coverage in inoculated regions of the agar (the rectangular regions shown in panel B) after contact with dirty (black) or cleaned (white) coatings. Error bars represent standard deviations of four independent trials.

reasons for this reduction in initial fouling on **AS1** are unclear; however, the percent areal coverage on all four coatings after cleaning was low and statistically similar. These quantitative results support the view that coatings **AS2**−**AS4** can be fouled using the repetitive physical contact methods used here, and that all four coatings can be easily cleaned under these conditions. We note here that that this contact-based agar plate method of analysis relies upon the transfer of bacteria from a contaminated coating to the agar plate (Figure 1A), and thus, the surface properties of the coatings (e.g., hydrophobicity,

https://doi.org/10.1021/acsomega.4c11020
ACS Omega 2025, 10, 7295−7305

wettability, etc.) could impact how effectively bacteria are transferred from the coating to the plate for analysis. Nevertheless, we interpret the results shown in Figure 1B,C to provide useful indirect measures of relative levels of contamination, and to provide support for the easy cleanability of coatings **AS1**−**AS4** using gentle and touch-free water-washing procedures. In the section below, we report the results of additional experiments using direct measures of bacterial attachment that reveal additional quantitative differences in the ability of coatings **AS1**−**AS4** to resist initial biofouling and/or allow for facile cleaning after repeated, longer-term fouling.

Quantitative Characterization of Bacterial Fouling and Cleaning after Repeated and Longer-Term Contact with Flowing Bacterial Culture. We performed a second series of experiments to characterize and quantify levels of initial bacterial contamination and subsequent cleaning of coatings **AS1**−**AS4** after multiple rounds of prolonged contact with a continuous flow of bacterial culture. For these experiments, we also used *S. aureus* AH1677 to allow for comparisons with the short-term assay above. We note that this strain produces yellow fluorescent protein (YFP), which facilitated visualization and quantitation using microscopy.[53] A peristaltic pump was used to continuously flow and recycle bacterial culture over the surfaces of coated substrates held at a fixed angle (Figure 2A). After 3 h of continuous inoculation, these substrates ("dirty" samples) were imaged by fluorescence microscopy and then rinsed gently and in a touch-free manner by dipping them consecutively, without agitation, into four separate containers of water containing no detergents or surfactants. The samples were then allowed to air-dry, and these "cleaned" samples were imaged again using fluorescence microscopy and the level of fluorescence quantified via computer image analysis. This general experimental setup allowed for the controlled, repeatable inoculation of all coatings repeatedly and under identical experimental conditions, including time, flow rate, and angle of flow. For the experiments described below, all coatings were exposed to 10 cycles of repeated inoculation and cleaning.

Figure 2B shows a schematic of a fouled substrate arising from these experiments showing fouled and unfouled regions used for subsequent image analysis by fluorescence microscopy and quantification of bacterial fouling. Figure 2B also shows representative digital photographs of substrates coated with **AS1** and **AS3** after one cycle of fouling and cleaning. Figure 3 shows representative fluorescence microscopy images acquired in the fouled regions of coatings **AS1**−**AS4** after fouling and cleaning for the first and tenth cycle, and reveals bacterial fouling to vary substantially, for both conditions, as a function of coating type.

We used computer image analysis to calculate average CTCF values for dirty and cleaned samples after each cycle (see Materials and Methods for additional details). The results of this analysis for cycles 1 and 10 are shown in Figure 2C,D. Inspection of these results reveals substrates coated with **AS3** to strongly prevent initial biofouling, relative to **AS1**, **AS2**, and **AS4**, for the first 3 h fouling and cleaning cycle (Figure 2C). Coatings **AS1**, **AS2**, and **AS4** all exhibited substantial fouling after one cycle but were all also easily cleaned by gentle water rinsing. In general, coatings containing higher amounts of hydrophobic polysiloxane segments (**AS3** and **AS4**) showed levels of fluorescence, after one cycle of fouling and cleaning, that were significantly lower than those for **AS1**, which does not contain polysiloxane segments. The resistance of **AS3** to initial fouling gradually eroded over subsequent fouling and cleaning cycles, reaching levels similar to those of **AS1**, **AS2**, and **AS4** after 10 fouling and cleaning cycles, (see Figure 2D and additional discussion below). Interestingly, however, substrates coated with **AS3** remained easier to clean (p <

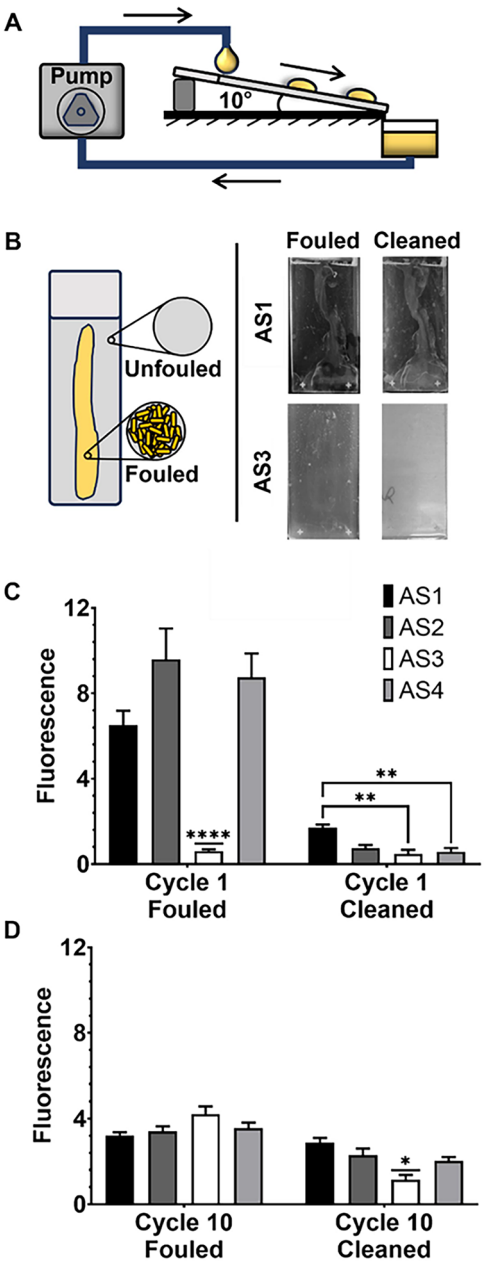

Figure 2. (A) Schematic showing the experimental approach used to expose coated substrates to a continuous flow of bacterial culture. (B) Left: Schematic showing a substrate after the fouling assay, showing a fouled region and surrounding nonfouled regions used as background during analysis of surface fouling. Right: Representative photographs of glass slides coated with **AS1** and **AS3** after one treatment with a culture of *S. aureus* ("fouled") and after gentle water-washing ("cleaned"). (C, D) Median CTCF values for coated substrates after 1 cycle (C) and 10 cycles (D) of fouling and cleaning with cultures of *S. aureus*. Error bars represent 95% confidence intervals for the median of three substrates for each coating type. Significance is shown as (* = $p < 0.05$; ** = $p < 0.01$; **** = $p < 0.0001$). Where noted with a single line, **AS3** (white bars) shows significantly lower fluorescence values than all other substrates tested.

https://doi.org/10.1021/acsomega.4c11020
ACS Omega 2025, 10, 7295−7305

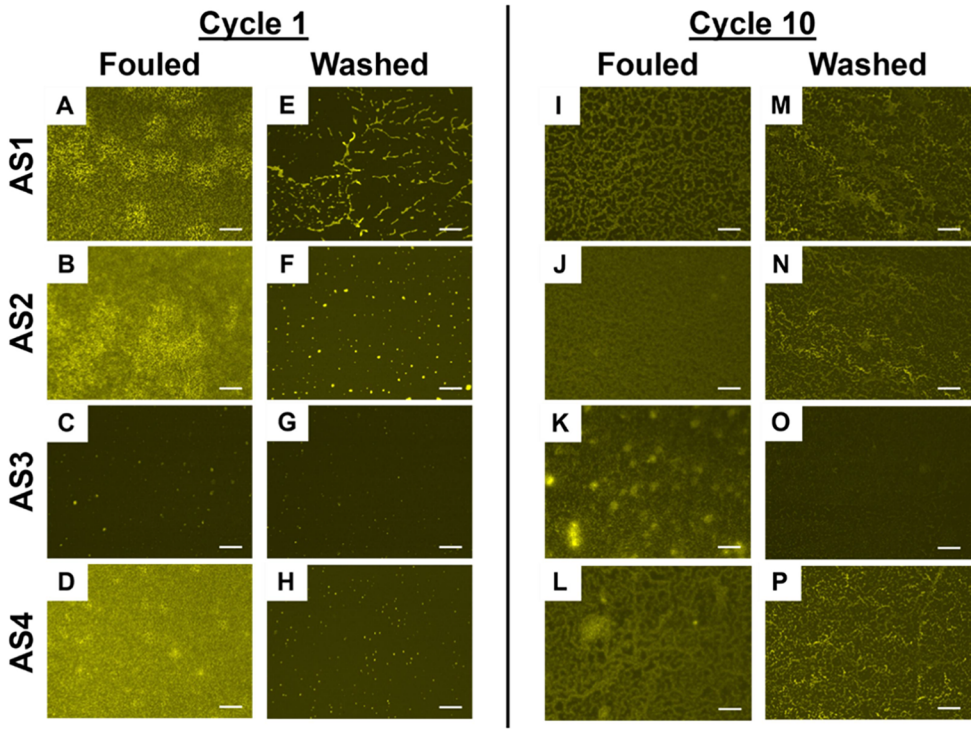

Figure 3. Representative fluorescence microscopy images of glass substrates coated with **AS1**−**AS4** after fouling/cleaning cycles consisting of 3 h of inoculation with *S. aureus* and subsequent cleaning with a gentle water rinse (see text). Left: (A−H) Results for fouled (A−D) and cleaned (E−H) coatings after one cycle of fouling and cleaning. Right: (I−P) Results for fouled (I−L) and cleaned (M−P) coatings after 10 cycles of fouling and cleaning. These images were used to generate the quantitative results shown in Figure 2C,D. All images are false-colored yellow; scale bars are 50 μm.

0.05) than these other coatings after repeated fouling for up to 10 cycles. Additional plots showing CTCF values for fouled and cleaned substrates for all 10 cycles of this experiment can be found in Figures S5 and S6 of the Supporting Information. Inspection of those additional results reveals **AS4** to exhibit levels of fluorescence after cleaning that were significantly lower than those of **AS1** for up to four cycles (Figure S6).

As shown in Table 1, **AS3** and **AS4** exhibit advancing water contact angles that are higher and values of contact angle hysteresis that are substantially lower than **AS1** and **AS2**. During the first cycle of fouling and cleaning, we observed the aqueous bacterial culture pumped across the more hydrophobic surfaces of **AS3** and **AS4** to break up and form droplets that rolled easily down the surfaces of coated substrates (e.g., Figure 2A); in contrast, aqueous culture formed a more continuous stream of fluid and pooled in larger areas at the bottoms of substrates coated with **AS1** and **AS2**. These quantitative differences in the surface wetting behaviors of **AS3** and **AS4** are consistent with the large differences in contact angle hysteresis relative to those of **AS1** and **AS2**. We note that the contact angle hysteresis for **AS3** (4.7 ± 1.9) was significantly lower than that of **AS4** (11.1 ± 0.5), consistent with the reduced amounts of initial fouling observed on **AS3** during the first cycle of fouling and cleaning. Additional characterization of surface roughness using stylus profilometry (Figure S7) indicated that differences in surface roughness were not correlated with observations of bacterial fouling after cleaning. We note, however, that contact angle hysteresis is determined, at least in part, by the combined influences of both surface roughness and surface chemistry, the latter of which is also additionally impacted here by the inclusion of siloxane-containing segments in these clearcoat materials.

The apparent wetting behaviors of **AS3** and **AS4** became less pronounced and more similar to those of **AS1** and **AS2** over time and with additional cycles of fouling and cleaning, consistent with the results of the fluorescence microscopy results discussed above and shown in Figure 2C. We note here that the fluorescence microscopy results summarized in Figure 2C reflect the ability of each of these coatings to prevent fouling by, and facilitate the subsequent removal of, fluorescent live and/or dead bacterial cells, which was the primary focus of this study. These results do not provide direct measures of fouling and/or removal of other non-fluorescent material, including components of media or other bacterial products that could affect changes in the wetting behaviors of these coatings after repeated exposure to fouling and cleaning cycles. Changes in the wetting behaviors of these substrates upon repeated cycling resulted in pumped streams of bacterial culture spreading more widely on the surfaces of the coatings and, in view of the constant fluid flow rates used in these experiments, a concomitant decrease in bacterial density in fouled regions during fouling cycles. Consistent with these observations, levels of fluorescence become more uniform across all coatings after fouling for 10 cycles (see Figures 2D and 3I−L), with no significant difference between any of the four coatings.

Overall, we conclude on the basis of the results above that **AS3** exhibits levels of bacterial fluorescence after cleaning that are small but significantly lower ($p < 0.05$) than those of coatings **AS1**, **AS2**, and **AS4** after 10 cycles of fouling and cleaning cycles using *S. aureus*. The results of additional experiments demonstrated that hydrophobic coatings **AS3** and **AS4** were also able to substantially reduce fouling by *E. coli*, a common Gram-negative bacterium, relative to **AS1** and **AS2**.

https://doi.org/10.1021/acsomega.4c11020
ACS Omega 2025, 10, 7295−7305

These experiments were conducted using the same general fluid-flow assay described above and a well-characterized *E. coli* strain (25922GFP) that constitutively produces green fluorescent protein (GFP). Inspection of Figure 4 reveals

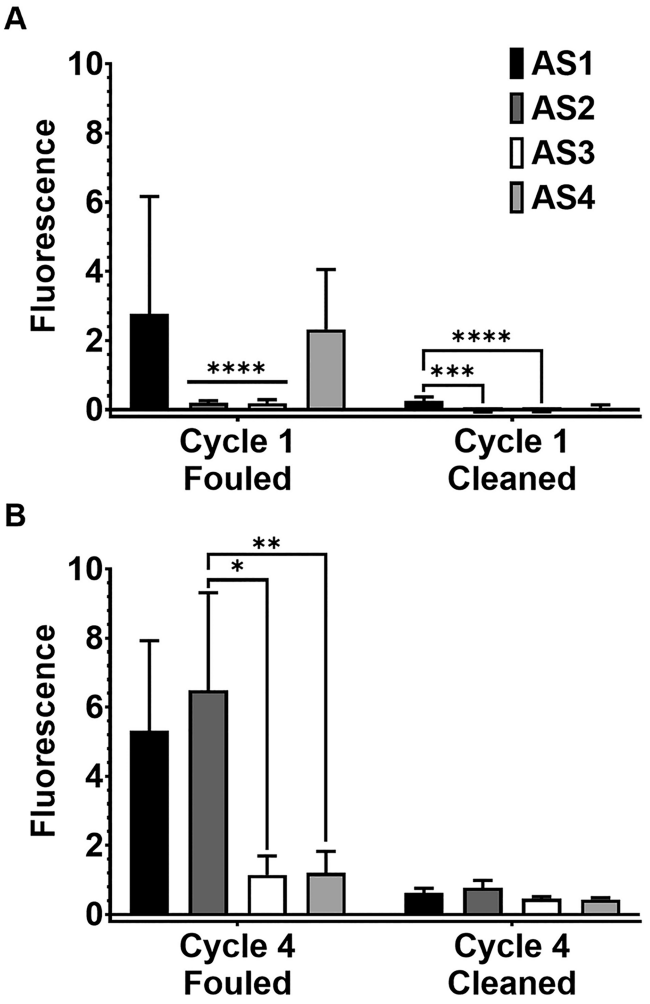

Figure 4. Median CTCF values for coated substrates after 1 cycle (A) and 4 cycles (B) of fouling and cleaning with cultures of *E. coli*. Error bars represent 95% confidence intervals for the median of three substrates for each coating type. Significance is shown as (* = $p < 0.05$; ** = $p < 0.01$; *** = $p < 0.001$; **** = $p < 0.0001$).

AS3 and **AS4** to exhibit reduced initial fouling as compared to **AS1** and **AS2** after at least four cycles. We note, however, that, in contrast to results described above using *S. aureus*, all four coatings exhibited low and similar levels of *E. coli*-associated fluorescence after four fouling and cleaning cycles under the conditions used here (that is, coatings **AS3** and **AS4** are able to substantially reduce initial fouling relative to **AS1** and **AS2**, but **AS1** and **AS2** are also readily cleared of *E. coli*-associated fluorescence under the conditions used here). Representative fluorescence microscopy images for substrates fouled with *E. coli* after one and four fouling and cleaning cycles can be found in Figure S4 in the Supporting Information. Differences in the levels of fouling by *E. coli* as compared to *S. aureus* are likely a result of differences in adhesion between the two species, at least under the conditions used in these experiments; for example, we are aware that this specific *S. aureus* strain is well-known to readily colonize surfaces and form biofilm.[53] Additional experiments will be needed to understand these differences and, more broadly, to screen these materials over a range of other time scales and conditions. Nevertheless, we conclude based on these current studies that **AS3** and **AS4** are both significantly more resistant to initial fouling by *E. coli*, a behavior that again correlates with the substantially lower contact angle hystereses for these coatings.

SUMMARY AND CONCLUSIONS

The results reported here demonstrate that the incorporation of hydrophobic polysiloxane segments into commercially relevant polyurethane coatings can significantly reduce initial biofouling by bacteria and facilitate the subsequent removal of adherent bacteria. We developed two microbiological assays to characterize polyurethane coatings **AS1**−**AS4** after repeated exposure to *S. aureus* and *E. coli* under (i) short-term, touch-based and (ii) longer-term, flow-based conditions, followed by gentle washing with water. Our results demonstrate that, in general, coatings **AS3** and **AS4**, which contain greater amounts of polysiloxane segments, exhibited lower degrees of initial fouling and/or were more easily cleaned after fouling in longer-term flow-based assays, as compared to coatings **AS1** and **AS2**. These results are consistent with the significantly lower contact angle hystereses of these more hydrophobic materials and suggest principles that may be useful to help guide the design of new classes of easy-to-clean polyurethane coatings for a range of commercial applications, including for use in high touch environments where bacterial fouling is common. The studies reported here evaluated fouling and cleaning using two bacteria that are common in commercial and clinical settings. We anticipate that the behaviors observed here will be general for several other types of Gram-positive and Gram-negative bacteria. Additional studies to evaluate fouling and cleaning of these coatings on other applied surfaces and using other cleaning methods are underway and will be reported separately.

ASSOCIATED CONTENT

Supporting Information

The Supporting Information is available free of charge at https://pubs.acs.org/doi/10.1021/acsomega.4c11020.

Additional microscopy images, plots, and digital photographs used to characterize the adhesion and subsequent removal of bacteria from coated substrates (PDF)

AUTHOR INFORMATION

Corresponding Authors

Visham Appadoo − *PPG Industries, Inc., Coating Innovation Center, Allison Park, Pennsylvania 15101, United States*; Email: vappadoo@ppg.com

Cornelius O. Audu − *PPG Industries, Inc., Coating Innovation Center, Allison Park, Pennsylvania 15101, United States*; Email: caudu@ppg.com

Helen E. Blackwell − *Department of Chemistry, University of Wisconsin−Madison, Madison, Wisconsin 53706, United States*; orcid.org/0000-0003-4261-8194; Email: blackwell@chem.wisc.edu

David M. Lynn − *Department of Chemical and Biological Engineering, University of Wisconsin−Madison, Madison, Wisconsin 53706, United States; Department of Chemistry, University of Wisconsin−Madison, Madison, Wisconsin*

https://doi.org/10.1021/acsomega.4c11020
ACS Omega 2025, 10, 7295−7305

53706, United States; orcid.org/0000-0002-3140-8637; Email: dlynn@engr.wisc.edu

Authors

Lawrence M. Chen − *Department of Chemical and Biological Engineering, University of Wisconsin−Madison, Madison, Wisconsin 53706, United States*

La'Darious J. Quinn − *Department of Chemistry, University of Wisconsin−Madison, Madison, Wisconsin 53706, United States*

Jordan T. York − *Department of Chemistry, University of Wisconsin−Madison, Madison, Wisconsin 53706, United States*

Thomas J. Polaske − *Department of Chemistry, University of Wisconsin−Madison, Madison, Wisconsin 53706, United States*

Alexandra E. Nelson − *Department of Chemistry, University of Wisconsin−Madison, Madison, Wisconsin 53706, United States*

Complete contact information is available at: https://pubs.acs.org/10.1021/acsomega.4c11020

Author Contributions

‖L.M.C. and L.J.Q. contributed equally.

Notes

The authors declare no competing financial interest.

■ ACKNOWLEDGMENTS

This research was sponsored by the U.S. Army Research Laboratory (ARL) and was accomplished under Cooperative Agreement Number W911NF2120028. The views and conclusions contained in this document are those of the authors and should not be interpreted as representing the official policies, either expressed or implied, of the U.S. Army Research Laboratory. The U.S. Government is authorized to reproduce and distribute reprints for Government purposes notwithstanding any copyright notation herein. L.J.Q., L.M.C., and T.J.P. were partially supported by the UW−Madison NIH Chemistry-Biology Interface Training Program (T32 GM008505). J.T.Y. was partially supported by the UW−Madison NIH Biotechnology Training Program (T32 GM135066). We thank A. Horswill (University of Colorado Medical School) for the generous donation of *S. aureus* strains. C.O.A. and V.A. would like to acknowledge PPG associates Abdulrahman Ibrahim, David Walters, Kerianne Dobosz, Kristin Nuzzio, and Melinda Dent for helpful discussions on the project and the data presented in this manuscript, and Christian Ruud for performing experiments to evaluate the surface morphology of the PPG coatings.

■ REFERENCES

(1) Zander, Z. K.; Becker, M. L. Antimicrobial and Antifouling Strategies for Polymeric Medical Devices. *ACS Macro Lett.* **2018**, *7* (1), 16−25.

(2) Wu, P.; Grainger, D. W. Drug/device combinations for local drug therapies and infection prophylaxis. *Biomaterials* **2006**, *27* (11), 2450−2467.

(3) Banerjee, I.; Pangule, R. C.; Kane, R. S. Antifouling coatings: recent developments in the design of surfaces that prevent fouling by proteins, bacteria, and marine organisms. *Adv. Mater.* **2011**, *23* (6), 690−718.

(4) Hetrick, E. M.; Schoenfisch, M. H. Reducing implant-related infections: Active release strategies. *Chem. Soc. Rev.* **2006**, *35* (9), 780−789.

(5) Campoccia, D.; Montanaro, L.; Arciola, C. R. A review of the biomaterials technologies for infection-resistant surfaces. *Biomaterials* **2013**, *34* (34), 8533−8554.

(6) Wei, T.; Yu, Q.; Chen, H. Responsive and Synergistic Antibacterial Coatings: Fighting against Bacteria in a Smart and Effective Way. *Adv. Healthcare Mater.* **2019**, *8* (3), No. e1801381.

(7) Flemming, H.-C.; Murthy, P. S.; Venkatesan, R.; Cooksey, K. E. *Marine and Industrial Biofouling*, 1st ed.; Springer, 2009.

(8) Lejars, M.; Margaillan, A.; Bressy, C. Fouling release coatings: A nontoxic alternative to biocidal antifouling coatings. *Chem. Rev.* **2012**, *112* (8), 4347−4390.

(9) Muthukrishnan, T.; Dobretsov, S.; De Stefano, M.; Abed, R. M. M.; Kidd, B.; Finnie, A. A. Diatom communities on commercial biocidal fouling control coatings after one year of immersion in the marine environment. *Marine Environmental Research* **2017**, *129*, 102−112.

(10) Ciriminna, R.; Bright, F. V.; Pagliaro, M. Ecofriendly Antifouling Marine Coatings. *ACS Sustainable Chem. Eng.* **2015**, *3*, 559−565.

(11) Lejeune, B. T.; Zhang, X.; Sun, S.; Hines, J.; Jinn, K. W.; Reilly, A. N.; Clark, H. A.; Lewis, L. H. Enhancing Biocidal Capability in Cuprite Coatings. *ACS Biomater Sci. Eng.* **2023**, *9* (7), 4178−4186.

(12) Makal, U.; Wood, L.; Ohman, D. E.; Wynne, K. J. Polyurethane biocidal polymeric surface modifiers. *Biomaterials* **2006**, *27* (8), 1316−1326.

(13) Kugela, A.; Stafslien, S.; Chisholma, B. J. Antimicrobial coatings produced by "tethering" biocides to the coating matrix: A comprehensive review. *Prog. Org. Coat.* **2011**, *72*, 222−252.

(14) Shi, X.; Zhang, R.; Sand, W.; Mathivanan, K.; Zhang, Y.; Wang, N.; Duan, J.; Hou, B. Comprehensive Review on the Use of Biocides in Microbiologically Influenced Corrosion. *Microorganisms* **2023**, *11* (9), 2194.

(15) Nir, S.; Reches, M. Bio-inspired antifouling approaches: The quest towards non-toxic and non-biocidal materials. *Curr. Opin Biotechnol* **2016**, *39*, 48−55.

(16) Jungnickel, C.; Stock, F.; Brandsch, T.; Ranke, J. Risk assessment of biocides in roof paint. Part 1: Experimental determination and modelling of biocide leaching from roof paint. *Environ. Sci. Pollut Res. Int.* **2008**, *15* (3), 258−265.

(17) Benn, T.; Cavanagh, B.; Hristovski, K.; Posner, J. D.; Westerhoff, P. The release of nanosilver from consumer products used in the home. *J. Environ. Qual* **2010**, *39* (6), 1875−1882.

(18) Park, M. S.; Kim, Y. D.; Kim, B. M.; Kim, Y. J.; Kim, J. K.; Rhee, J. S. Effects of Antifouling Biocides on Molecular and Biochemical Defense System in the Gill of the Pacific Oyster *Crassostrea gigas*. *PLoS One* **2016**, *11*, No. e0168978.

(19) Ferrari, M.; Benedetti, A. Superhydrophobic surfaces for applications in seawater. *Adv. Colloid Interface Sci.* **2015**, *222*, 291−304.

(20) Epstein, A. K.; Wong, T.-S.; Belisle, R. A.; Boggs, E. M.; Aizenberg, J. Liquid-infused structured surfaces with exceptional anti-biofouling performance. *Proc. Natl. Acad. Sci. U. S. A.* **2012**, *109* (33), 13182−13187.

(21) Xiao, L. L.; Li, J. S.; Mieszkin, S.; Di Fino, A.; Clare, A. S.; Callow, M. E.; Callow, J. A.; Grunze, M.; Rosenhahn, A.; Levkin, P. A. Slippery Liquid-Infused Porous Surfaces Showing Marine Antibiofouling Properties. *Acs Appl. Mater. Inter* **2013**, *5* (20), 10074−10080.

(22) Sokolova, A.; Cilz, N.; Daniels, J.; Stafslien, S. J.; Brewer, L. H.; Wendt, D. E.; Bright, F. V.; Detty, M. R. A comparison of the antifouling/foul-release characteristics of non-biocidal xerogel and commercial coatings toward micro- and macrofouling organisms. *Biofouling* **2012**, *28* (5), 511−523.

(23) Sethi, S. K.; Manik, G. Recent Progress in Super Hydrophobic/Hydrophilic Self-Cleaning Surfaces for Various Industrial Applications: A Review. *Polym.-Plast. Technol. Eng.* **2018**, *57* (18), 1932−1952.

(24) Wong, T.-S.; Kang, S. H.; Tang, S. K. Y.; Smythe, E. J.; Hatton, B. D.; Grinthal, A.; Aizenberg, J. Bioinspired self-repairing slippery

surfaces with pressure-stable omniphobicity. *Nature* **2011**, *477* (7365), 443−447.
(25) Anand, S.; Paxson, A. T.; Dhiman, R.; Smith, J. D.; Varanasi, K. K. Enhanced Condensation on Lubricant-Impregnated Nanotextured Surfaces. *ACS Nano* **2012**, *6* (11), 10122−10129.
(26) Lafuma, A.; Quéré, D. Slippery pre-suffused surfaces. *EPL (Europhysics Letters)* **2011**, *96* (5), 56001.
(27) Sotiri, I.; Overton, J. C.; Waterhouse, A.; Howell, C. Immobilized liquid layers: A new approach to anti-adhesion surfaces for medical applications. *Exp. Biol. Med.* **2016**, *241* (9), 909−918.
(28) Howell, C.; Grinthal, A.; Sunny, S.; Aizenberg, M.; Aizenberg, J. Designing Liquid-Infused Surfaces for Medical Applications: A Review. *Adv. Mater.* **2018**, *30*, No. 1802724.
(29) Solomon, B. R.; Subramanyam, S. B.; Farnham, T. A.; Khalil, K. S.; Anand, S.; Varanasi, K. K., Chapter 10 Lubricant-Impregnated Surfaces. In *Non-wettable Surfaces: Theory, Preparation and Applications*; The Royal Society of Chemistry, 2017; pp 285−318.
(30) Privett, B. J.; Youn, J.; Hong, S. A.; Lee, J.; Han, J.; Shin, J. H.; Schoenfisch, M. H. Antibacterial Fluorinated Silica Colloid Superhydrophobic Surfaces. *Langmuir* **2011**, *27* (15), 9597−9601.
(31) Esmeryan, K. D.; Castano, C. E.; Chaushev, T. A.; Mohammadi, R. Silver-doped superhydrophobic carbon soot coatings with enhanced wear resistance and anti-microbial performance. *Colloids Surf., A* **2019**, *582*, No. 123880.
(32) Esmeryan, K. D.; Chaushev, T. A. Anti-biofouling potential of extremely water-repellent carbon soot coatings immersed in a highly-contaminated seawater swamp. *Prog. Org. Coat.* **2023**, *183*, No. 107719.
(33) Lin, Y.; Zhang, H.; Zou, Y.; Lu, K.; Li, L.; Wu, Y.; Cheng, J.; Zhang, Y.; Chen, H.; Yu, Q. Superhydrophobic photothermal coatings based on candle soot for prevention of biofilm formation. *J. Mater. Sci. Technol.* **2023**, *132*, 18−26.
(34) Ragesh, P.; Ganesh, V. A.; Naira, S. V.; Nair, A. S. A review on 'self-cleaning and multifunctional materials'. *J. Mater. Chem. A* **2014**, *2* (36), 14773−14797.
(35) Zhao, J.; Zhang, T.; Li, Y.; Huang, L.; Tang, Y. Fluorine-Free, Highly Durable Waterproof and Breathable Fibrous Membrane with Self-Clean Performance. *Nanomaterials* **2023**, *13* (3), 516.
(36) Zhang, J.; Zhang, L.; Gong, X. Large-Scale Spraying Fabrication of Robust Fluorine-Free Superhydrophobic Coatings Based on Dual-Sized Silica Particles for Effective Antipollution and Strong Buoyancy. *Langmuir* **2021**, *37* (19), 6042−6051.
(37) Sethi, S. K.; Shankar, U.; Manik, G. Fabrication and characterization of non-fluoro based transparent easy-clean coating formulations optimized from molecular dynamics simulation. *Prog. Org. Coat.* **2019**, *136*, No. 105306.
(38) Maayan, M.; Mani, K. A.; Yaakov, N.; Natan, M.; Jacobi, G.; Atkins, A.; Zelinger, E.; Fallik, E.; Banin, E.; Mechrez, G. Fluorine-Free Superhydrophobic Coating with Antibiofilm Properties Based on Pickering Emulsion Templating. *ACS Appl. Mater. Interfaces* **2021**, *13*, 37693−37703.
(39) Buck, M. E.; Breitbach, A. S.; Belgrade, S. K.; Blackwell, H. E.; Lynn, D. M. Chemical modification of reactive multilayered films fabricated from poly(2-alkenyl azlactone)s: Design of surfaces that prevent or promote mammalian cell adhesion and bacterial biofilm growth. *Biomacromolecules* **2009**, *10* (6), 1564−1574.
(40) Breitbach, A. S.; Broderick, A. H.; Jewell, C. M.; Gunasekaran, S.; Lin, Q.; Lynn, D. M.; Blackwell, H. E. Surface-mediated release of a synthetic small-molecule modulator of bacterial quorum sensing: gradual release enhances activity. *Chem. Commun.* **2011**, *47* (1), 370−372.
(41) Broderick, A. H.; Breitbach, A. S.; Frei, R.; Blackwell, H. E.; Lynn, D. M. Surface-mediated release of a small-molecule modulator of bacterial biofilm formation:A non-bactericidal approach to inhibiting biofilm formation in *Pseudomonas aeruginosa*. *Adv. Healthc Mater.* **2013**, *2* (7), 993−1000.
(42) Broderick, A. H.; Stacy, D. M.; Tal-Gan, Y.; Kratochvil, M. J.; Blackwell, H. E.; Lynn, D. M. Surface coatings that promote rapid release of peptide-based AgrC inhibitors for attenuation of quorum sensing in *Staphylococcus aureus*. *Adv. Healthc Mater.* **2014**, *3* (1), 97−105.
(43) Kratochvil, M. J.; Tal-Gan, Y.; Yang, T.; Blackwell, H. E.; Lynn, D. M. Nanoporous Superhydrophobic Coatings that Promote the Extended Release of Water-Labile Quorum Sensing Inhibitors and Enable Long-Term Modulation of Quorum Sensing in *Staphylococcus aureus*. *ACS Biomater Sci. Eng.* **2015**, *1* (10), 1039−1049.
(44) Kratochvil, M. J.; Welsh, M. A.; Manna, U.; Ortiz, B. J.; Blackwell, H. E.; Lynn, D. M. Slippery Liquid-Infused Porous Surfaces that Prevent Bacterial Surface Fouling and Inhibit Virulence Phenotypes in Surrounding Planktonic Cells. *ACS Infect Dis* **2016**, *2* (7), 509−517.
(45) Kratochvil, M. J.; Yang, T.; Blackwell, H. E.; Lynn, D. M. Nonwoven Polymer Nanofiber Coatings That Inhibit Quorum Sensing in *Staphylococcus aureus*: Toward New Nonbactericidal Approaches to Infection Control. *ACS Infect. Dis.* **2017**, *3* (4), 271−280.
(46) Manna, U.; Raman, N.; Welsh, M. A.; Zayas-Gonzalez, Y. M.; Blackwell, H. E.; Palecek, S. P.; Lynn, D. M. Slippery Liquid-Infused Porous Surfaces that Prevent Microbial Surface Fouling and Kill Non-Adherent Pathogens in Surrounding Media: A Controlled Release Approach. *Adv. Funct Mater.* **2016**, *26* (21), 3599−3611.
(47) Agarwal, H.; Nyffeler, K. E.; Blackwell, H. E.; Lynn, D. M. Fabrication of Slippery Liquid-Infused Coatings in Flexible Narrow-Bore Tubing. *ACS Appl. Mater. Interfaces* **2021**, *13* (46), 55621−55632.
(48) Agarwal, H.; Polaske, T. J.; Sanchez-Velazquez, G.; Blackwell, H. E.; Lynn, D. M. Slippery nanoemulsion-infused porous surfaces (SNIPS): Anti-fouling coatings that can host and sustain the release of water-soluble agents. *Chem. Commun.* **2021**, *57* (94), 12691−12694.
(49) Agarwal, H.; Quinn, L. J.; Walter, S. C.; Polaske, T. J.; Chang, D. H.; Palecek, S. P.; Blackwell, H. E.; Lynn, D. M. Slippery Antifouling Polymer Coatings Fabricated Entirely from Biodegradable and Biocompatible Components. *ACS Appl. Mater. Interfaces* **2022**, *14* (15), 17940−17949.
(50) Agarwal, H.; Nyffeler, K. E.; Manna, U.; Blackwell, H. E.; Lynn, D. M. Liquid Crystal-Infused Porous Polymer Surfaces: A "Slippery" Soft Material Platform for the Naked-Eye Detection and Discrimination of Amphiphilic Species. *ACS Appl. Mater. Interfaces* **2021**, *13* (28), 33652−33663.
(51) Swarup, S.; Xu, X.; Vanier, N.; Endlish, M.; Simpson, D. Acrylic polymers, curable film-forming compositions prepared therefrom, and method of mitigating dirt build-up on a substrate. U. S. Patent No. 9,120,916 B1, 2015.
(52) Schwendeman, J.; Swarup, S.; Endlish, M.; Xu, X. Curable film-forming compositions and method of mitigating dirt build-up on a substrate. U. S. Patent No. 9,187,670 B1, 2015.
(53) Kirchdoerfer, R. N.; Garner, A. L.; Flack, C. E.; Mee, J. M.; Horswill, A. R.; Janda, K. D.; Kaufmann, G. F.; Wilson, I. A. Structural basis for ligand recognition and discrimination of a quorum-quenching antibody. *J. Biol. Chem.* **2011**, *286* (19), 17351−17358.
(54) Owens, D. K.; Wendt, R. C. Estimation of Surface Free Energy of Polymers. *J. Appl. Polym. Sci.* **1969**, *13* (8), 1741.
(55) Issa, M. W.; Barancyk, S. V.; Rock, R. M.; Gilchrist, J. F.; Wirth, C. L. Impact of resin molecular weight on drying kinetics and sag of coatings. *Prog. Org. Coat.* **2024**, *194*, No. 108618.
(56) Rabea, A. M.; Mohseni, M.; Mirabedini, S. M.; Tabatabaei, M. H. Surface analysis and anti-graffiti behavior of a weathered polyurethane-based coating embedded with hydrophobic nano silica. *Appl. Surf. Sci.* **2012**, *258*, 4391−4396.
(57) ASTM Standard D5296-19. *Standard Test Method for Molecular Weight Averages and Molecular Weight Distribution of Polystyrene by High Performance Size-Exclusion Chromatography*; ASTM International: West Conshohocken, PA, 2019.
(58) ASTM Standard D4274-11. *Standard Test Methods for Testing Polyurethane Raw Materials: Determination of Hydroxyl Numbers of Polyols*; ASTM International: West Conshohocken, PA, 2011.
(59) Fox, R. B.; Bitner, J. L.; Hinkley, J. A.; Carter, W. Dynamic Mechanical Properties of Some Polyurethane-Acrylic Copolymer

https://doi.org/10.1021/acsomega.4c11020
ACS Omega 2025, 10, 7295−7305

Interpenetrating Polymer Networks. *Polym. Eng. Sci.* **1985**, *25* (3), 157−163.
(60) Soldera, A.; Metatla, N. Glass transition of polymers: Atomistic simulation versus experiments. *Phys. Rev. E* **2006**, *74*, No. 061803.
(61) Tal-Gan, Y.; Stacy, D. M.; Foegen, M. K.; Koenig, D. W.; Blackwell, H. E. Highly potent inhibitors of quorum sensing in *Staphylococcus aureus* revealed through a systematic synthetic study of the group-III autoinducing peptide. *J. Am. Chem. Soc.* **2013**, *135* (21), 7869−7882.
(62) Tal-Gan, Y.; Ivancic, M.; Cornilescu, G.; Cornilescu, C. C.; Blackwell, H. E. Structural characterization of native autoinducing peptides and abiotic analogues reveals key features essential for activation and inhibition of an AgrC quorum sensing receptor in *Staphylococcus aureus*. *J. Am. Chem. Soc.* **2013**, *135* (149), 18436−18444.

https://doi.org/10.1021/acsomega.4c11020
ACS Omega 2025, 10, 7295−7305